Resistance to Mass Transfer Inside Droplets

A. H. P. SKELLAND and R. M. WELLEK

Illinois Institute of Technology, Chicago, Illinois

An experimental investigation of the effects of various physical properties on the dispersed-phase mass transfer coefficient was carried out for both nonoscillating and oscillating liquid droplets falling in a single stream through stationary continuous liquid phases. The Colburn and Welsh two-component technique was used to isolate and measure the dispersed-phase resistance to mass transfer. This technique limited the experimental study to systems with low interfacial tensions, between 2.5 and 5.8 dynes/cm. Solute was transferred into the droplets, and the droplet concentration was measured after droplet-fall heights ranging from about 2 cm. to 103 cm. Precautions were taken to minimize end effects.

The experimental mass transfer rates on nonoscillating droplets in general were greater than that predicted by the Kronig and Brink model for nonoscillating circulating droplets. Experimental Sherwood numbers for four liquid systems were correlated in terms of a relationship involving the dispersed-phase Schmidt number, the Weber number, and the time group, $4D_Lt_c/d^2_e$, which allows for the time dependency of the transfer mechanism. The data were correlated with an average absolute deviation of 34%. The Kronig and Brink and Newman relations fitted the experimental data for nonoscillating droplets with an average absolute deviation of 46 and 54%, respectively. The experimental results for the oscillating droplets were correlated by two relationships with an average absolute deviation of 10.5%. The Handlos and Baron model fitted the experimental results for oscillating droplets with an average absolute deviation of 38%.

Liquid-liquid extraction is one of the important chemical engineering operations. Many types of equipment have been designed for this operation: packed columns, mixer-settlers, spray columns, perforated-plate columns and others. In spray and perforated-plate columns, mass transfer occurs between a liquid continuous phase and a dispersed phase of liquid droplets. There are at least three major periods in the droplet life during which mass transfer takes place: (1) during formation of the droplets in the continuous phase, (2) during free rise or fall of the droplets through this continuous phase, and (3) during coalescence of the droplets at the end of the free-rise period.

Period (2) is of prime importance in spray columns. Periods (1) and (3) may be of more importance than period (2) in a perforated-plate column, particularly if there are many stages (*3, 9, 23, 28*). In this work, only the mass transfer occurring during period (2) has been studied.

Considerable work has been reported on the correlation of the continuous phase resistance to mass transfer. Much of this material is summarized in references *13, 25* and *29*. Garner and Tayeban (*8*) separated the effects of oscillating and nonoscillating droplets on the resistance offered by the continuous phase.

These findings, with the present work on dispersed-phase resistance, should contribute toward the ultimate objective of the design of extraction columns from rate relationships, without the need for experimentally determined efficiencies. The detailed procedure is to be published later.

PREVIOUS WORK AND THEORETICAL CONSIDERATIONS

For drops which are internally stagnant and with no resistance in the continuous phase, Newman's (*26*) theoretical expression leads to

$$k_d = -\frac{d}{6t}\ln\frac{6}{\pi^2}\sum_{n=1}^{\infty}\left[\frac{1}{n^2}\exp\left(-\frac{n^2 D_L \pi^2 t}{(d/2)^2}\right)\right] \quad (1)$$

When transfer resistance is zero in the continuous phase and laminar circulation exists inside the drop, Kronig and Brink's (*21*) expression leads to

$$k_d = -\frac{d}{6t}\ln\frac{3}{8}\sum_{n=1}^{\infty}\left[B_n^2\exp\left(-\lambda_n\frac{16\,D_I t}{(d/2)^2}\right)\right] \quad (2)$$

B_n and λ_n are given by Heertjes et al. (*17*) for $1 \leq n \leq 7$ and Elzinga and Banchero (*5*) for $1 \leq n \leq 3$.

Handlos and Baron (*16*) proposed a mechanism in which a form of turbulence due to assumed random radial motions is superimposed on circulation within the drop. Their expressions are for zero resistance in the continuous phase and lead to

$$k_d = -\frac{d}{6t}\ln 2\sum_{n=1}^{\infty}\left[B_n\exp\left(-\frac{\lambda_n\,16\,D_I t\,N_{Pe'}}{2048\,d^2}\right)\right] \quad (3)$$

Previous workers (*8, 17, 19*) have compared their measurements of dispersed-phase resistance (a total of eight different systems) with one or another of these three theoretical models. For stagnant drops there is good agreement with the Newman relationship. Some circulating drops have shown good agreement with the Kronig and Brink expression although notable exceptions occurred for the *n*-butanol-water system. Results for the oscillating droplets deviated significantly from the Handlos and Baron model.

APPARATUS AND EXPERIMENTAL PROCEDURE

The purpose of the apparatus is to disperse a single stream of liquid drops into a liquid continuous phase. The dispersed-phase fluid was stored in a 50 cc. constant-head buret (A) (Figure 1), fitted with a Teflon needle valve (B) which eliminates the problem of contamination with stopcock grease. The needle valve is designed for use with a range of nozzle sizes (C). The larger nozzles were made of thin-walled glass tubing with the tip ground so that the plane of the tip was at right angles to the axis of the nozzle. These were attached

A. H. P. Skelland is at Notre Dame University, Notre Dame, Indiana. R. M. Wellek is at the Missouri School of Mines and Metallurgy, Rolla, Missouri.

Table 1. Physical Properties

System	Composition	ρ_d, g./cc.	ρ_c, g./cc.	μ_d, centipoise	μ_c, centipoise	σ,* dyne/cm.	X_d, weight percent	X_c,	T, °C.	D_L,† sq. cm./sec. × 10^5
Water and ethyl acetate	Pure	0.9968	0.8945	0.885	0.445				25.6	0.89
	sat.	0.9957	0.899	1.060	0.460	5.78	7.44	3.33		
Ethyl acetoacetate and water	Pure	1.0194	0.9970	1.495	0.895				25.0	1.26
	sat.	1.0220	1.0054	1.580	1.130	3.50	6.06	11.5		
Glycol diacetate and water	Pure	1.0990	0.9971	2.62	0.917				24.2	0.756
	sat.	1.0976	1.0226	2.44	1.350	2.33	8.73	14.9		
Glyceryl triacetate and water	Pure	1.1531	0.9971	10.9	0.910				24.7	0.146
	sat.	1.1472	1.0002	16.6	0.935	3.99	4.86	5.5		

* Phases mutually saturated.
† Calculated from Olander's modification of Wilke-Chang correlation.

directly to the Teflon needle valve with glass connectors. The smaller nozzles were stainless steel hypodermic needles with the tips ground to a sharp, conical edge.

Pyrex glass extraction columns (E) were used which had an inside diameter of about 7.5 cm. and effective height of 14, 28, 54, 78 and 103 cm. At the bottom of each column was a conical section from which the droplets were removed for analysis. The exit flow rate was controlled by means of a Teflon needle valve (F) at the bottom of the column.

Materials

The Colburn and Welsh (2) two-component technique was used in this study. The two most important requirements for this procedure are that the saturation concentration in the continuous phase must not be high or there will be a significant resistance in this phase, and that the saturation concentration in the dispersed phase must be large enough to obtain a measurable rate of mass transfer.

The systems studied, with the dispersed phase mentioned first, are water-ethyl acetate, ethyl acetoacetate-water, glycol diacetate-water and glyceryl triacetate-water.

Because surface-active agents can have a profound effect on the mass transfer mechanism, considerable attention was given to ensuring the purity of all liquids used in the experiments. All organic liquids were purified by vacuum distillation in an all-glass still with a reflux column. Only the middle cut (about 75% of the total) was used in the mass transfer and eccentricity experiments. All connections in the distillation apparatus were made by means of ground glass joints. The laboratory distilled water was redistilled in an all-glass distillation flask.

Physical Properties

Densities were measured with pycnometers, viscosities with a u-tube viscometer, and interfacial tensions with a ring tensiometer. The interfacial tension was measured between mutually saturated phases, in view of the usual assumption of interfacial equilibrium in two-phase transfer. Mutual solubilities of the two-component systems were determined by the conventional titration procedure.

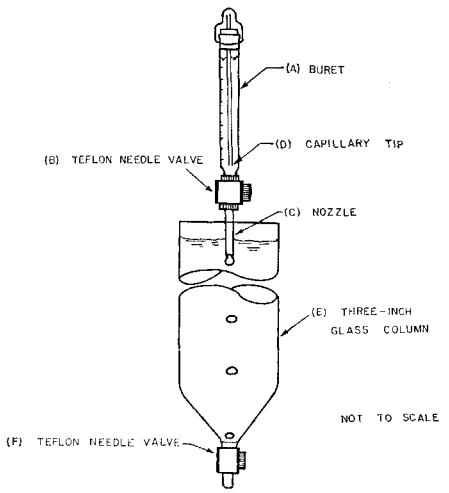

Fig. 1. Diagram of apparatus for mass transfer experiments.

The saturation concentration of the continuous-phase liquid in the dispersed phase was determined with more precision than the concentration of the dispersed-phase liquid in the continuous phase. This is because the saturation concentration in the dispersed phase is used to calculate the dispersed-phase mass transfer coefficient. The continuous-phase saturation concentration was determined only to ensure that it was not more than about 15%, by mass, which has been considered the maximum permissible for the Colburn and Welsh technique to be of value (6).

Diffusivities were calculated by the Wilke-Chang correlation (30) which was adjusted using the Olander modification (27) when water was the solute.

Physical properties appear in Table 1.

Procedure: Mass Transfer

Droplets were formed at a frequency of 10 drops/15 sec. for all but the ethyl acetoacetate-water system, for which the frequency was 5 drops/15 sec. Between 5 and 15 cc. of dispersed phase were passed through the column in each run. A further 7 to 10 cc. of dispersed phase were passed through the column before each run during the start-up period and discarded before sampling began. The outlet valve at the foot of the column was adjusted to give an interface at the very apex of the cone. This eliminated inclusion of slugs of continuous phase when withdrawing the coalesced droplets and minimized transfer across the coalesced interface.

Droplet-fall velocities were obtained with an electric timer accurate to ± 0.005 sec. for a free-fall distance of 45 or 65.5 cm.

Concentrations were determined by refractive index with a previously determined calibration curve.

The average drop volume in a given run was calculated from the measured duration of the run, the total volume of dispersed phase used, and the frequency of drop formation. The time from droplet detachment at the nozzle to arrival at the coalesced layer was measured in order to calculate the time of contact during the free-fall period, t_c.

Calculation of dispersed-phase coefficient of mass transfer, k_d

A differential material balance on the dispersed-phase results in the following expression which defines the inside transfer coefficient:

$$\frac{d}{dt} VC = k_d (C_i - C) A \qquad (4)$$

where C is the average solute concentration in the droplet. When the two-component technique of Colburn and Welsh is used and equilibrium between the phases at the interface is assumed, the concentrations of each phase immediately adjacent to the interface are equal to the saturation concentration of each phase:

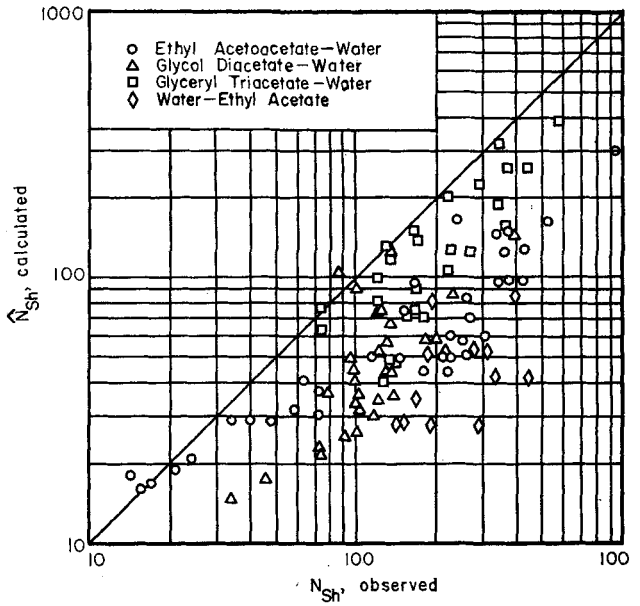

Fig. 2. Newman model, nonoscillating droplets.

$$C_i = C, \text{ saturation}$$

Thus, the interfacial concentrations are constant (for a constant temperature and pressure) and are easily determined from measurements of the saturation solubility. There is one disadvantage in using the Colburn and Welsh technique which is not always mentioned in the literature. The partially miscible binary systems in general have low interfacial tensions. Thus, if it is desired to test or obtain a mass transfer correlation for high interfacial tension systems, another technique must be used. It has also been stated that two-component systems do not exhibit the complicating factors (for example, interfacial turbulence) that have been observed for three component systems (*4*).

Since the object of this work was to study the mass transfer mechanism during the free-fall period, it was necessary to eliminate or minimize the effects of mass transfer during droplet formation and coalescence. As an example of these effects, after a 2.0 cm. fall period, the total fractional extraction in ethyl acetoacetate droplets was 0.12 and 0.36 for equivalent droplet diameters of 0.95 cm. and 0.30 cm., respectively. For a column height of 78.0 cm., the total fractional extraction for the above two droplet sizes increased to 0.43 and 0.64, respectively.

At present no reliable method has been found for entirely eliminating end effects. Thus the original graphical extrapolation procedure to zero column height used by Sherwood, Evans, and Longcor (*28*) and by Licht and Conway (*23*), using a plot of the log fraction solute unextracted vs. drop-fall time or column height, has been shown to be invalid by Licht and Pansing (*24*).

The more sophisticated graphical extrapolation techniques of Johnson and Hamielec, et al. (*19, 20*) can only be used in those cases in which the data yield straight lines when plotted in their special manner. This condition was not fulfilled sufficiently to use the method in our case.

The technique used in this work to correct for end effects is described as follows. In order to reduce the transfer to the coalesced drops, the interfacial area of the coalesced layer was kept very small (about ½ sq. cm.). The coalescence end effect is reduced to a minimum; therefore the solute concentration in the exit stream closely approximates the average concentration of the droplet just before it lands at the coalesced layer. Hence, the droplet concentration after withdrawal from the shortest column approximately equals that after the same length of fall in any longer column. The average droplet concentration during the free fall in any longer column was then considered to vary from the exit concentration of the shortest column, C_o, to the exit concentration from any longer column, C_f. The corresponding time of contact was the difference between the total fall times in the shortest column and any longer column, that is, $t_f - t_o$. With these boundary conditions on the droplet concentration and time of contact, Equation (4) was integrated to give the following expression for k_d:

$$k_d = -\frac{V}{A}\frac{1}{(t_f - t_o)} \ln\frac{C_i - C_f}{C_i - C_o} \tag{5}$$

if

$$t_c = t_f - t_o$$

and

$$E_m = \frac{C_f - C_o}{C_i - C_o}$$

then

$$k_d = -\frac{V}{A\,t_c} \ln(1 - E_m) \tag{6}$$

The method used in this work is identical with that used by Garner, Foord and Tayeban (*6*), Garner and Tayeban (*8*), and Garner and Skelland (*12*). This method, described above, definitely eliminates transfer occurring during formation and detachment of the drop, leaving only the question of transfer during withdrawal of the drops at the end of the column (a significant coalescence interface is not present in this method). Transfer during withdrawal was assumed to be negligible in similar work by Calderbank and Korchinski (*1*) on droplet heat transfer, and the results of this assumption agreed well with theoretical predictions. Our technique regarding end effects is, therefore, at least in line with that used by several other workers.

The interfacial area A in Equation (6) was calculated as the surface of a sphere and as the surface of an oblate spheroid with the same volume as the droplet in both cases. The area of the spheroid was readily calculated from that of the sphere using the relationship presented by Garner and Tayeban (*8*).

Droplet Eccentricity

Eccentricity is defined in this work as d_h/d_v. Droplets were photographed during free fall through a 7.6 cm. I.D. glass column with a central viewing section made of optically plane glass to eliminate distortion effects. Eccentricities were measured from enlarged projections of these photographs. Measurements were made in two separate sets, one in which the phases were mutually saturated and the other in which the dispersed phase was initially pure before introduction to the column.

RESULTS: MASS TRANSFER

The experimental results were divided into two categories, nonoscillating droplets and oscillating droplets.

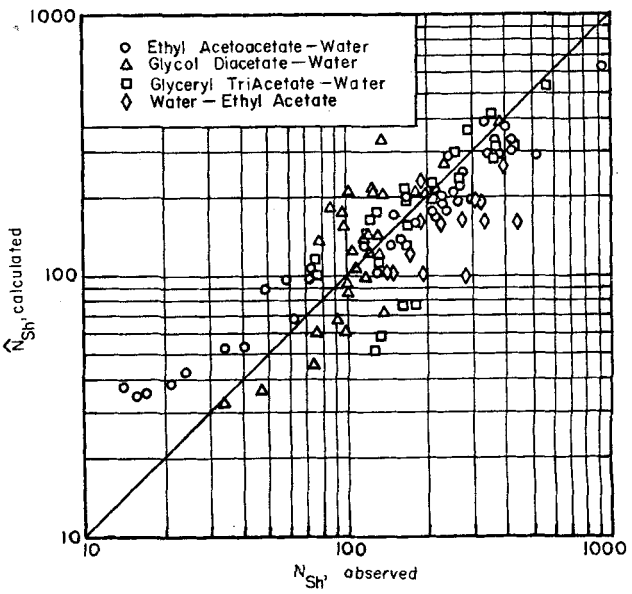

Fig. 3. Kronig and Brink model, nonoscillating droplets.

The original data are deposited with the A.D.I.*

Sherwood numbers were calculated from the experimental k_d values by multiplying by d_e/D_L. The values for the nonoscillating droplets are compared with the theoretical Sherwood numbers obtained from Equations (1) and (2) for stagnant droplets and for circulating droplets as shown in Figures 2 and 3, respectively.

A similar comparison for oscillating droplets appears in Figure 4, where the Sherwood number is obtained from Equation (3) for droplets which are both circulating and oscillating.

Nonoscillating Droplets

The discrepancies between experimental and theoretical N_{Sh} values in Figure 2 indicate that circulation currents were present inside most of the droplets used in this study. Figure 3 further shows that the rate of transfer very often exceeds that predicted for circulating droplets by the Kronig and Brink relation, even though no visible oscillation of these droplets could be detected. It may be noted, however, that the Kronig and Brink relationship was derived for conditions in which the circulation patterns within the drop are those given by Hadamard (*14*). These patterns in turn are restricted to the Stokesian regime of flow (that is, $N_{Re} < 1$). Nevertheless, Hamielec and Johnson (*15*) indicate theoretically that the Hadamard circulation patterns may be approximated under certain conditions up to Reynolds numbers of about 80. The droplet Reynolds number range in the present work was 37 to 546.

An empirical correlation of the results for nonoscillating droplets was, therefore, attempted. Both the Newman and the Kronig and Brink models [Equations (1) and (2)] consider the internal mass transfer coefficient to be a function of only 3 variables:

$$k_d = f\,(t_c, D_L, d_e) \tag{7}$$

It appeared from graphical representations of the data and past observations on droplet phenomena (*7, 10, 11*) that the function probably should include other variables. The following function expresses those which are possibly relevant:

$$k_d = f_N\,(t_c, D_L, d_e\,U, \mu_c, \mu_d, \rho_c, \rho_d, \sigma) \tag{8}$$

The data were correlated by twelve dimensionless variants of Equation (8), using the least squares technique which has been programmed for use on the IBM-1620 digital computer (*22*). Three further correlation forms were tested, in which k_d was based on the true area of the ellipsoidal droplets. In one of these forms, d_e was the diameter of the sphere of the same volume. In the other two forms, d_e was the average of the major and minor axes of the ellipsoid. The best correlation from the fifteen examined was as follows:

$$\hat{N}_{Sh} = 31.4\,N_{T_m}^{-0.338}\,N_{Sc}^{-0.125}\,N_{We}^{0.371} \tag{9}$$

N_{Tm} is a dimensionless time group which appears in the theoretical expressions of Newman and Kronig and Brink. It contains the time of contact, t_c, and thereby makes some allowance for the unsteady state nature of the mechanism.

The average absolute deviation of the data from this equation is 34%, the estimate of variance, S^2 (log $\hat{N}_{Sh}$), is 0.035, and the multiple regression coefficient, R, is 0.83. The confidence limits of the exponents at the 95% probability level are:

$$-0.338 \pm 0.075;\ -0.125 \pm 0.024;\ 0.371 \pm 0.12$$

Experimental inaccuracies suggest rounding off of these exponents to two decimal places.

Equation (9) is for systems with low interfacial tensions (2.34-4.8 dynes/cm.) and low continuous-phase viscosities ($\mu_c < 1.35$ centipoise). It covers the following range of variables:

14.2	$\leq$	N_{Sh}	$\leq$	934
0.03×10^{-3}	$\leq$	N_{Tm}	$\leq$	32×10^{-3}
856	$\leq$	N_{Sc}	$\leq$	79,800
0.48	$\leq$	N_{We}	$\leq$	7.6

Values calculated from Equation (9) are compared with experimental values in Figure 5. The estimate of the variance and the average absolute deviation of this correlation

* Tabular material has been deposited as document 7923 with the American Documentation Institute, Photoduplication Service, Library of Congress, Washington 25, D. C., and may be obtained for $3.75 for photoprints or $2.00 for 35-mm. microfilm.

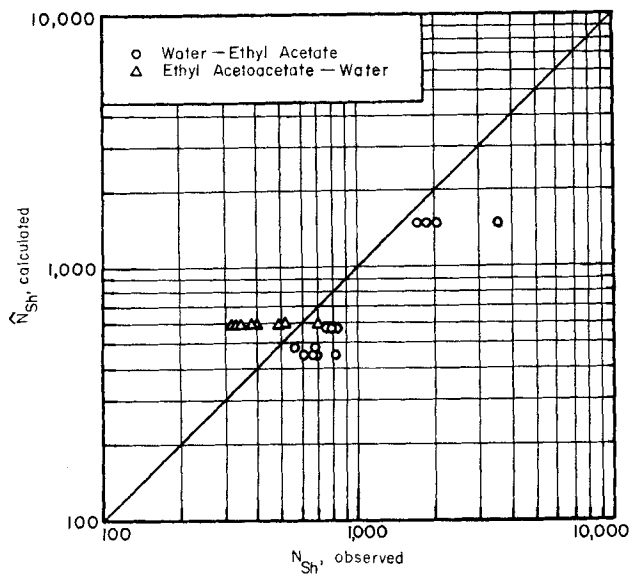

Fig. 4. Handlos and Baron model, oscillating droplets.

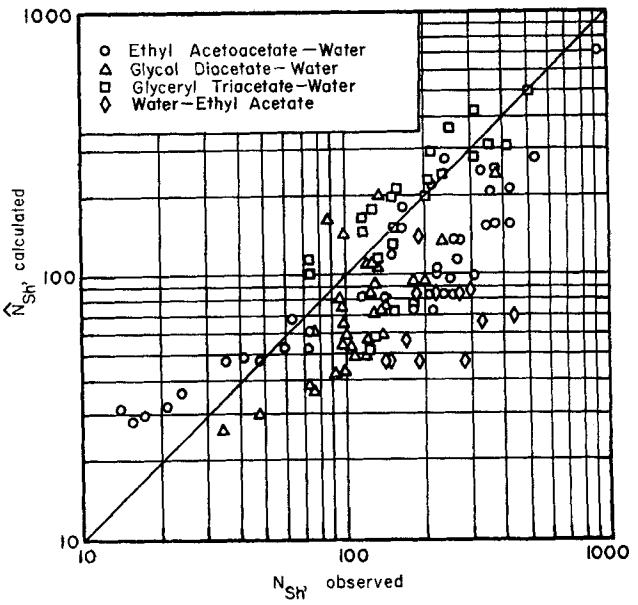

Fig. 5. Equation (9), nonoscillating droplets, $\hat{N}_{Sh} = 31.4\,N_{Tm}^{-0.338}\,N_{Sc}^{-0.125}We^{0.371}$.

are compared with those of the theoretical relationships of Newman (stagnant drops) and Kronig and Brink (circulating drops) as follows:

	% Average Absolute deviation	S^2 $(\log \hat{N}_{Sh})$
Equation (9)	34	0.035
Newman	54	4.94
Kronig and Brink	46	0.092

Oscillating Droplets

The transition from nonoscillating droplets occurred at a Reynolds number of about 600 for the water-ethyl acetate system and 360 for the ethyl acetoacetate-water system.

The correlating procedure for oscillating droplets was similar to that described for nonoscillating droplets. From seventeen correlating forms examined, two alternative equations were ultimately found to fit the data about equally well and are as follows:

$$\hat{N}_{Sh} = 0.320\, N_{Tm}^{-0.141}\, N_{Re}^{0.683}\, N_p^{0.10} \qquad (10)$$

$$\hat{N}_{Sh} = 0.142\, N_{Tm}^{-0.141}\, N_{We}^{0.769}\, N_p^{0.285} \qquad (11)$$

N_p is the P group which was used with success by Hu and Kintner (*18*) in correlating droplet-fall velocity with a variety of variables.

The average absolute deviation for Equations (10) and (11) is 10.5%; $S^2(\log \hat{N}_{Sh})$ for Equations (10) and (11) is equal to 0.0042. The multiple regression coefficient R for both equations is 0.97.

The confidence limits of the exponents at the 95% probability level are:

-0.141 ± 0.060	-0.141 ± 0.059
0.684 ± 0.220	0.760 ± 0.246
0.100 ± 0.078	0.285 ± 0.042

The data on which Equations (10) and (11) are based are for systems of low interfacial tensions (3.5-5.8 dynes/cm.) and low continuous-phase viscosities ($\mu_c < 1.35$ centipoise). The range of variables is:

326	$\leq$	N_{Sh}	$\leq$ 3,650
0.0097×10^{-3}	$\leq$	N_{Tm}	$\leq 2.19 \times 10^{-3}$
411	$\leq$	N_{Re}	$\leq$ 3114
1.78×10^{8}	$\leq$	N_p	$\leq 37.2 \times 10^{8}$
6.38	$\leq$	N_{We}	$\leq$ 13.3

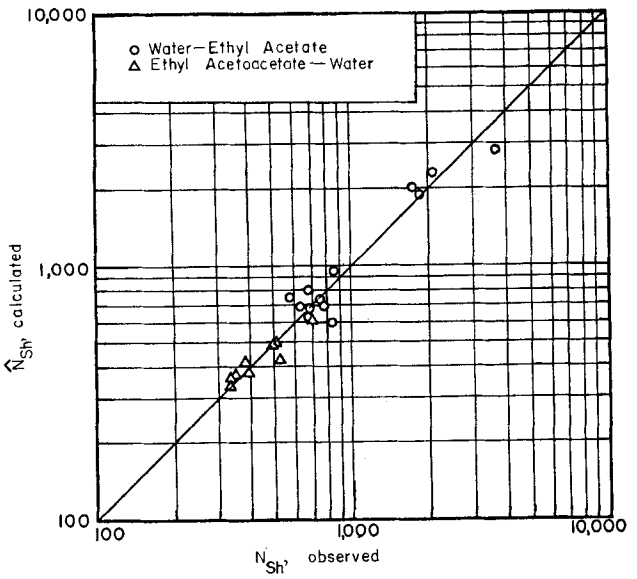

Fig. 6. Equation (11), oscillating droplets, $\hat{N}_{Sh} = 0.142\, N_{Tm}^{-0.141}\, We^{0.769}\, N_p^{0.285}$.

Values calculated from Equation (11) are compared with the experimental values in Figure 6. Equation (10) yields a closely similar plot.

The estimate of the variance and the average absolute deviation of these correlations are compared with those for the theoretical relationships of Handlos and Baron (circulating and oscillating drops) as follows:

	% Average Absolute deviation	S^2 $(\log \hat{N}_{Sh})$
Equation (10)	10.5	0.0042
Equation (11)	10.5	0.0042
Handlos and Baron	38.3	0.040

ACKNOWLEDGMENT

The financial support of the Sinclair Oil and Refining Company in the form of a Fellowship and of the National Science Foundation in the form of a summer Fellowship, both to R. M. Wellek, is gratefully acknowledged.

F. R. Anderson and R. F. Zabransky gave assistance in photographing the droplet profiles.

NOTATION

A = interfacial areas of droplet, sq. cm.
B_n = coefficients in series expansion
C = average solute concentration in the droplet, g. mole/cc.
C_i = solute concentration on the dispersed-phase side of the interface, g. mole/cc.
C_f, C_o = average solute concentration in the droplet at t_f and t_o, respectively, g. mole/cc.
d = diameter of spherical droplet, cm.
d_e = diameter of sphere having the same volume as the droplet, cm.
d_h = length of horizontal axis of droplet, cm.
d_v = length of vertical axis of droplet, cm.
D_L = molecular diffusivity of solute in dispersed phase, sq. cm./sec.
E_m = fractional extraction
f, f_n = functions
g = acceleration of gravity, cm./sq. sec.
k_d, $\hat{k}_d$ = dispersed-phase mass transfer coefficient, observed and calculated, respectively, g. mole/(sec.) (sq. cm.) (g. mole/cc.)
N_{Re} = Reynolds number, $d_e U \rho_c / \mu_c$
N_{Sc} = dispersed-phase Schmidt number, $\mu_d / \rho_d D_L$
N_{Sh}, $\hat{N}_{Sh}$ = Sherwood number observed and calculated, respectively, $\frac{k_d d_e}{D_L}$, $\frac{\hat{k}_d d_e}{D_L}$
N_P = P group, $\frac{\sigma^3 \rho_c^2}{g \mu_c^4 \Delta\rho}$
N_{We} = Weber number, $d_e U^2 \rho_c / \sigma$
$N_{\mu R}$ = viscosity ratio, μ_d / μ_c
N_{Tm} = dimensionless time group, $4 D_L t_c / d_e$
$N_{Pe'}$ = modified Peclet group, $N_{Re} N_{Sh} / (1 + N_{\mu R})$

$S^2(\log \hat{N}_{Sh})$ = estimate of variance of $\log \hat{N}_{Sh}$
t = time of contact, sec.
t_c = time of contact during free fall
t_o = time of fall for the shortest distance (from detachment at the nozzle to arrival at the coalesced layer), sec.
t_f = time of fall for any other fall distance, sec.
T = temperature, °C.
U = gross terminal velocity of droplet, cm./sec.
V = volume of droplet, cc.
X_d = weight percentage of continuous phase in dispersed phase
X_c = weight percentage of dispersed phase in continuous phase
λ_n = eigenvalues
μ_c, μ_d = viscosity of continuous and dispersed phase, respectively, poise
ρ_c, ρ_d = density of continuous and dispersed phase, g./cc.
σ = interfacial tension, dynes/cm.

LITERATURE CITED

1. Calderbank, P. H., and I. J. O. Korchinski, *Chem. Eng. Sci.*, **6**, 65 (1956).
2. Colburn, A. P., and D. B. Welsh, *Trans. Am. Inst. Chem. Engrs.*, **38**, 179 (1942).
3. Coulson. J. M., and S. J. Skinner, *Chem. Eng. Sci.*, **1**, 197 (1952).
4. Davies, J. T., *Trans. Inst. Chem. Engrs.*, **38**, 289 (1960).
5. Elzinga, E. R., and J. T. Banchero, *Chem. Eng. Progr. Symposium Ser. No. 29*, **55**, 149 (1959).
6. Garner, F. H., A. Foord, and M. Tayeban, *J. Appl. Chem.*, **9**, 315 (1959).
7. Garner, F. H., and P. J. Haycock, *Proc. Royal Soc.*, **A252**, 457 (1959).
8. ———, and M. Tayeban, *Anales de la Real Sociedad Espanola, de Fisica y Quimica*, Serie B-Quimica, Tomo LVI (B), 479 (1960).
9. ———, and A. H. P. Skelland, *Ind. Eng. Chem.*, **46**, 1255 (1954).
10. ————, *Chem. Eng. Sci.*, **4**, 149 (1955).
11. ————, *Trans. Inst. Chem. Engrs.*, (*London*), **29**, 315 (1951).
12. ————, *Ind. Eng. Chem.*, **48**, 51 (1956).
13. Griffith, R. M., *Chem. Eng. Sci.*, **12**, 198 (1960).
14. Hadamard, J., *Compt. Rend.*, **152**, 1735 (1911).
15. Hamielec, A. E., and A. I. Johnson, *Can. J. Chem. Eng.*, **4**, 41 (1962).
16. Handlos, A. E., and Thomas Baron, *A.I.Ch.E. Journal*, **3**, 127 (1957).
17. Heertjes, P. M., W. A. Holve, and H. Talsma, *Chem. Eng. Sci.*, **3**, 122 (1954).
18. Hu, Shengen, and R. C. Kintner, *A.I.Ch.E. Journal*, **1**, 42, (1955).
19. Johnson, A. I., and A. E. Hamielec, *ibid.*, **6**, 145 (1960).
20. ————, D. Wood, and A. Golding, *Can. J. Chem. Eng.*, 221 (1958).
21. Kronig, R., and J. C. Brink, *Appl. Sci. Res.*, **A-2**, 142 (1950).
22. Leeson, D., IBM-1620 Program Library, No. 6.0. 002, available prior to July (1962).
23. Licht, William, and J. B. Conway, *Ind. Eng. Chem.*, **42**, 1151 (1950).
24. ———, and W. F. Pansing, *ibid.*, **45**, 1855 (1953).
25. Linton, M., and K. L. Sutherland, *Chem. Eng. Sci.*, **12**, 214 (1960).
26. Newman, A. B., *Trans. Am. Inst. Chem. Engrs.*, **27**, 203 (1931).
27. Olander, D. R., *A.I.Ch.E. Journal*, **7**, 175 (1961).
28. Sherwood, T. K., J. E. Evans, and J. V. A. Longcor, *Ind. Eng. Chem.*, **31**, 1144 (1939).
29. Thorsen, G., and S. G. Terjesen, *Chem. Eng. Sci.*, **17**, 137 (1962).
30. Wilke, C. R., and Pen Chang, *A.I.Ch.E. Journal*, **1**, 264 (1955).

Manuscript received February 11, 1963; revision received November 18, 1963; paper accepted November 19, 1963. Paper presented at A.I.Ch.E. New Orleans meeting.

Selectivity in Hydrocarbon Oxidation

MAURICE SPIELMAN

Esso Research and Engineering Company, Madison, New Jersey

This article presents an analytical study of two reaction sequences postulated for liquid phase hydrocarbon oxidation. Major differences between reactor types are found. The relationship between conversion of feed and selectivity to intermediate product is strongly influenced by the type of reactor used. At any conversion level selectivity and yield of intermediate are higher in a batch or plug flow reactor than in a continuous flow stirred reactor.

The undesirable result of conversion beyond the point of maximum yield is also shown. Choice of an optimum conversion level is thus simplified.

Application of the calculated results to experimental data on ordinary and boric acid modified air oxidation of cyclohexane are given.

The results of this study are not limited to oxidation. They can provide a helpful tool for planning and interpreting experimental studies, for visualizing fundamental process limitations at an early stage of development, and for making maximum use of existing data.

In many chemical reactions of commercial interest the desired product is an intermediate in a sequence of reactions. For example in liquid phase hydrocarbon oxidations it is often found that overoxidation results in a host of useless and undesirable tars and condensation products. These degrade feedstock to waste value and often cause fouling and plugging in process vessels. On the other hand low conversion, underoxidation, reduces the amount of undesirable materials made but increases the complexity and cost of operation by requiring large equipment to handle high recycle rates.

Operating conditions selected are often those near the highest conversion possible without getting into process difficulties. In many cases optimization with respect to balancing the cost of recycle against the value of high selectivity to product is not adequately explored. By means of kinetic studies optimum conversion levels can be shown to be well below those usually considered normal.